

Contact Analysis between the Rotor and the Stator of a Progressive Cavity Pump

Mitrașcă Nușa*, Vlad Ulmanu** , Alexandru Pupăzescu**

* National Research - Development Institute for Oilfield Equipment – IPCUP Ploiesti
e-mail: nusamitrasca@yahoo.com

** Petroleum-Gas University of Ploiesti, Bd. București 39, Ploiești

Abstract

The wear what occurs between the stator and the rotor has an important role in the working life of progressive cavity pumps (PCP) in design parameters. In addition to the tribological characteristics of the materials of stator-rotor the great importance is the contact pressure between the two elements in relative motion. Initially this contact pressure is closely related to the type of rotor-stator assemblage, but it may also depend on other factors such as: modulus of elasticity, Poisson's ratio, coefficient of frictions etc. For this reason it is necessary to evaluate with precision enough contact pressure between the stator and rotor. In this paper are presented the results of the numerical analysis based on FEM for contact pressure depending on interference, physic and mechanical characteristics of the material of the stator and rotor.

Key words: *progressive cavity pomp, contact, FEM.*

Introduction

The fit of PCP way affect its performance. A too high interference involves high energy consumption and lead to rapid wear. An interference failure leads to a low PCP efficiency. For these reasons it is necessary to an analysis of stator-rotor contact. The analytical problem solving of the problem of contact within stator-rotor PCP involves many difficulties, both in terms of design, but also from the viewpoint of mathematical apparatus used [1,2]. An evaluation of it is using finite element method (FEM).

The Model

In the case of PCP was used to model a contact-type rigid-flexible. In order to simplify the problem, with consequences which are favorable to the convergence of the solution, it was considered a model plane of contact between stator and rotor of PCP, for their relative positions shown in Figure 1.

For this reason, the finite element items used was:

- in order to achieve the physical model of the stator of the PCP impeller was used the finite elements PLANE183 of finite element program ANSYS;
- for contact between the two parts of the PCP, we used elements of TARGE169 and CONTA172.

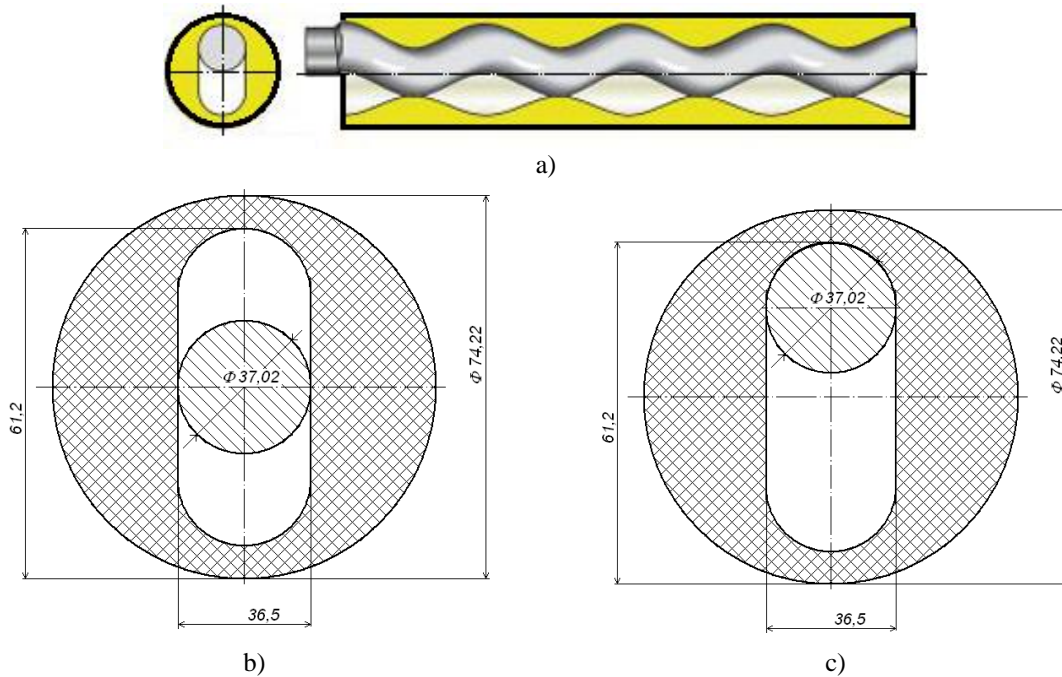


Fig. 1. The geometry and dimensions of the stator-rotor of PCP and the two relative positions analyzed.

These two models were solved for many situations, namely:

- different interferences;
- a specific interference and multiple values of the module of elasticity E_s of the material of stator of PCP;
- a specific interference and multiple values of the coefficient of the material pump μ of the material of stator of PCP;
- a specific interference and multiple values of the coefficient of friction between the stator and the rotor materials.

To solve the problem for the elastic deformations are required physical-mechanical characteristics of the two materials that is into contact: elastomer of stator and steel of rotor.

To determine for elastomer of stator the elasticity module and E_s and Poisson's coefficient μ_s determinations were carried out on specimens test subject to tensile and compression. On these specimens XY strain gauges was glued and the records was made with ESAM Static.

The tensile specimen had a rectangular section 22.5 x 9.3 mm x mm and 130 mm the length. The stress-strain diagram (fig. 2) was achieved without using strain gauges.

To determine the Poisson's coefficient were used strain gauges with very low load to protect them. Results and data processing are presented in tables 1 and 2. Based on these values were plotted graphs in Figures 2 and 3.

The stress-strain diagram (fig. 2) shows that the linearizing reaction occurs at higher stresses. Result the modulus of elasticity of the stator material $E_{s100} = 4.9\text{MPa}$. From the values presented in table 1 has been determined the value of the coefficient of Poisson: for tension $\mu_s^{\text{ten}} = 0.3671$ and $\mu_s^{\text{comp}} = 0.3919$ for compression.

Based on these results, in numerical analysis for the stator, we used the following physical-mechanical features: $E_s = 4.9 \dots 490 \text{ MPa}$ for longitudinal elasticity module and $\mu_s = 0.1 \dots 0.4$ to Poisson's ratio. For rotor $E = 2.05 \cdot 10^5 \text{ MPa}$ and $\mu = 0.3$, characteristic of steel. Were considered more interferences $j = 0.26 \dots 0.4 \text{ mm}$ tolerance field of the stator-rotor assemblage.

Table 1. The results of the tensile test for HBNR elastomer.

F , N	Δl , mm	σ , N/mm ²	A , %	F , N	Δl , mm	σ , N/mm ²	A , %
55.213	1.2888	0.26	0.99	1201.7	158.43	5.74	121.87
128.29	4.495	0.61	3.46	1223.9	161.63	5.85	124.33
181.31	7.7049	0.87	5.93	1247.5	164.83	5.96	126.79
228	10.912	1.09	8.39	1271.1	168.04	6.07	129.26
270.61	14.118	1.29	10.86	1294.4	171.24	6.19	131.72
308.79	17.322	1.48	13.32	1319.1	174.45	6.30	134.19
344.12	20.528	1.64	15.79	1343.2	177.65	6.42	136.65
376.45	23.733	1.80	18.26	1367.7	180.86	6.54	139.12
406.08	26.941	1.94	20.72	1393	184.07	6.66	141.59
433.66	30.151	2.07	23.19	1418.1	187.27	6.78	144.05
459.7	33.354	2.20	25.66	1443.5	190.47	6.90	146.52
483.9	36.562	2.31	28.12	1469.8	193.68	7.02	148.98
506.63	39.769	2.42	30.59	1495.6	196.89	7.15	151.45
528.17	42.976	2.52	33.06	1522.2	200.09	7.27	153.92
568.93	49.389	2.72	37.99	1575.4	206.5	7.53	158.85
588.26	52.595	2.81	40.46	1602.5	209.7	7.66	161.31
606.62	55.803	2.90	42.93	1630.2	212.9	7.79	163.77
624.67	59.012	2.99	45.39	1658	216.11	7.92	166.24
642.34	62.218	3.07	47.86	1686	219.32	8.06	168.71
659.62	65.425	3.15	50.33	1714.5	222.52	8.19	171.17
676.82	68.632	3.23	52.79	1742.9	225.72	8.33	173.63
693.9	71.841	3.32	55.26	1771.9	228.93	8.47	176.10
710.64	75.049	3.40	57.73	1800.5	232.13	8.60	178.56
727.43	78.257	3.48	60.20	1829.6	235.34	8.74	181.03
743.9	81.466	3.56	62.67	1858.9	238.54	8.88	183.49
760.8	84.675	3.64	65.13	1888.4	241.75	9.02	185.96
794.21	91.084	3.80	70.06	1947.8	248.15	9.31	190.88
811.01	94.293	3.88	72.53	1977.5	251.36	9.45	193.35
828.42	97.503	3.96	75.00	2008	254.56	9.60	195.82
845.42	100.71	4.04	77.47	2038.3	257.77	9.74	198.28
862.99	103.92	4.12	79.94	2068.9	260.98	9.89	200.75
880.94	107.13	4.21	82.41	2099.5	264.19	10.03	203.22
898.6	110.33	4.29	84.87	2130	267.4	10.18	205.69
916.92	113.55	4.38	87.35	2160.6	270.62	10.33	208.17
935.48	116.75	4.47	89.81	2192.1	273.83	10.48	210.64
954.26	119.96	4.56	92.28	2222.5	277.03	10.62	213.10
973.38	123.17	4.65	94.75	2253.8	280.25	10.77	215.58
992.55	126.38	4.74	97.22	2284.8	283.45	10.92	218.04
1011.6	129.58	4.83	99.68	2315.8	286.66	11.07	220.51
1031.5	132.79	4.93	102.15	2347.5	289.88	11.22	222.98
1051.8	135.99	5.03	104.61	2378.7	293.09	11.37	225.45
1072.1	139.2	5.12	107.08	2409.2	296.29	11.51	227.92
1092.8	142.41	5.22	109.55	2441.2	299.51	11.67	230.39
1113.8	145.61	5.32	112.01	2472.9	302.72	11.82	232.86
1135.3	148.81	5.43	114.47	2503.5	305.93	11.96	235.33
1156.9	152.02	5.53	116.94	2535.5	309.13	12.12	237.79
1179	155.22	5.63	119.40	2566.5	312.36	12.27	240.28

Table 2. The results for Poisson's coefficient for HBNR elastomer.

Tensile test					Compression test				
F, N	σ , MPa	Strain		μ_s	F, N	σ , MPa	Strain		μ_s
		ε_1 , $\mu\text{m/m}$	ε_2 , $\mu\text{m/m}$				ε_1 , $\mu\text{m/m}$	ε_2 , $\mu\text{m/m}$	
0.0000	0.0000	0	0	-	0.0000	0.0000	0	0	-
0.4332	0.0021	14.22	-5.212	0.3665	0.4746	0.0023	-6.27	3.763	0.6002
0.8371	0.0040	19.6	-7.219	0.3683	0.5679	0.0027	-7.77	4.391	0.5651
1.1882	0.0057	24.49	-8.724	0.3562	0.6612	0.0032	-9.53	4.642	0.4871
1.5179	0.0073	29.62	-10.229	0.3453	0.7545	0.0036	-10.78	5.394	0.5004
1.8476	0.0088	34.89	-12.236	0.3507	0.8478	0.0041	-12.53	6.021	0.4805
2.1774	0.0104	39.77	-14.244	0.3582	0.9411	0.0045	-14.16	6.021	0.4252
2.4975	0.0119	44.66	-16.251	0.3639	1.0343	0.0049	-15.91	7.025	0.4415
2.7865	0.0133	49.79	-18.007	0.3617	1.1276	0.0054	-17.42	7.401	0.4249
3.0755	0.0147	54.8	-19.261	0.3515	1.2209	0.0058	-19.55	8.656	0.4428
3.3642	0.0161	59.31	-22.272	0.3755	1.3142	0.0063	-20.55	8.53	0.4151
3.6529	0.0175	63.57	-23.777	0.3740	1.4417	0.0069	-22.05	8.656	0.3926
3.9416	0.0188	68.33	-25.282	0.3700	1.4288	0.0068	-23.68	9.157	0.3867
4.3289	0.0207	72.34	-28.042	0.3876	1.5185	0.0073	-25.31	8.656	0.3420
4.6081	0.0220	77.23	-29.296	0.3793	1.6081	0.0077	-26.69	9.157	0.3431
4.8873	0.0234	81.99	-29.798	0.3634	1.6978	0.0081	-28.44	9.534	0.3352
5.1571	0.0246	86.12	-31.429	0.3649	1.7874	0.0085	-29.57	10.286	0.3479
5.4151	0.0259	90.75	-33.31	0.3671	1.8771	0.0090	-31.07	10.788	0.3472
5.6732	0.0271	94.89	-35.317	0.3722	1.9668	0.0094	-32.32	12.043	0.3726
5.9312	0.0283	99.27	-37.074	0.3735	2.0564	0.0098	-33.7	12.168	0.3611
6.1893	0.0296	103.28	-37.952	0.3675	2.1461	0.0103	-35.58	12.921	0.3632
6.4471	0.0308	107.29	-39.833	0.3713	2.2357	0.0107	-36.83	13.297	0.3610
6.7026	0.0320	111.8	-41.088	0.3675	2.3254	0.0111	-37.96	13.673	0.3602
6.9581	0.0333	115.93	-42.593	0.3674	2.4151	0.0115	-39.09	13.799	0.3530
7.2137	0.0345	120.69	-43.847	0.3633	2.5047	0.0120	-40.72	14.3	0.3512
7.4692	0.0357	124.33	-44.976	0.3617	2.5944	0.0124	-41.59	14.426	0.3469
7.7248	0.0369	128.96	-46.607	0.3614	2.6840	0.0128	-42.85	14.928	0.3484
7.9803	0.0381	131.97	-48.112	0.3646	2.7737	0.0133	-44.1	15.931	0.3612
8.1506	0.0390	134.47	-49.116	0.3653	2.8634	0.0137	-44.98	15.931	0.3542
8.3210	0.0398	137.98	-50.245	0.3641	2.9530	0.0141	-46.35	16.433	0.3545
8.4914	0.0406	140.74	-51.374	0.3650	3.0427	0.0145	-47.61	16.433	0.3452
8.6617	0.0414	143.24	-52.628	0.3674	3.1323	0.0150	-48.98	17.436	0.3560
8.8321	0.0422	146.62	-53.632	0.3658	3.2220	0.0154	-50.24	17.687	0.3521
9.0024	0.0430	149.75	-54.635	0.3648	3.3117	0.0158	-51.61	18.189	0.3524
9.2580	0.0442	154.14	-55.89	0.3626	3.4013	0.0163	-52.62	18.691	0.3552

Results and Conclusions

Following the solutions program provides the following results: contact pressure (fig. 4), the contact stresses due to friction, total contact stresses, etc. The results obtained were plotted graphs in Figures 5 and 6.

From the analysis results, the following conclusions have emerged:

- Contact pressure increase with increasing interference (fig. 5,a). This ensures a good PCP efficiency but results in increased energy necessary operation the pump due to the rise of friction;

- Contact pressure increases rapidly with increasing the value of longitudinal elasticity module of material stator E_s , pump (fig. 5,b) and decreases with the increase of the coefficient of Poisson stator μ_s , (fig. 6,a). In order to achieve a good volumetric efficiency should therefore carry out an optimum between E_s and μ_s ;
- Contact pressure increase with the increase of the coefficient of friction between stator and rotor (fig. 6,b). It is therefore necessary to determine what influence the processing speed of the wear between the stator and the rotor.

It follows from the need for an accurate determination of the contact pressure between the rotor and stator of PCP on the one hand to determine the nature of the assemblage leading to a high volumetric efficiency and low energy consumption, and on the other hand to assess the speed of the wear of stator, i.e. the rotor.

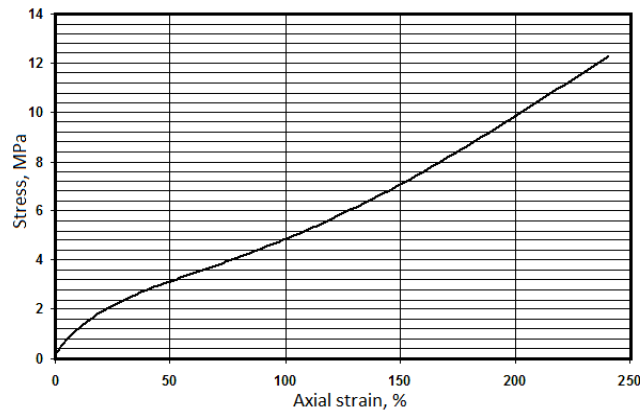


Fig. 2. The stress-strain diagram for HBNR elastomer

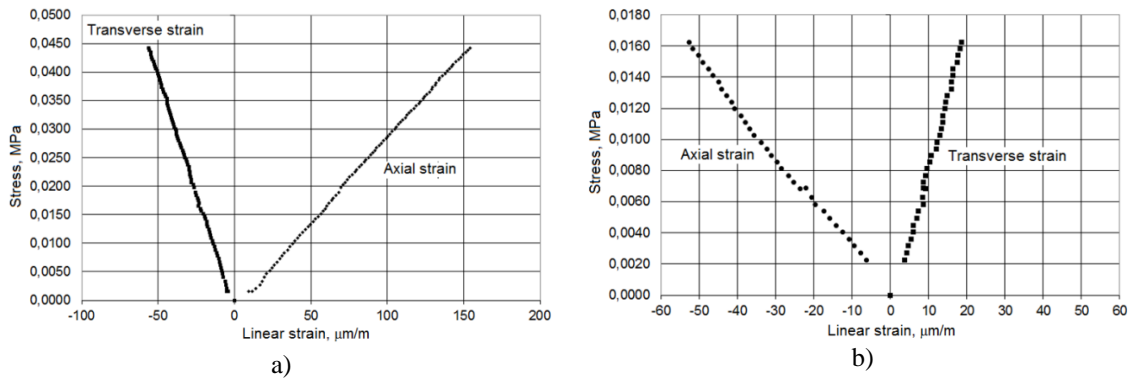


Fig. 3. Stress – strain correlation for HBNR elastomer: a) tensile test; b) compression test

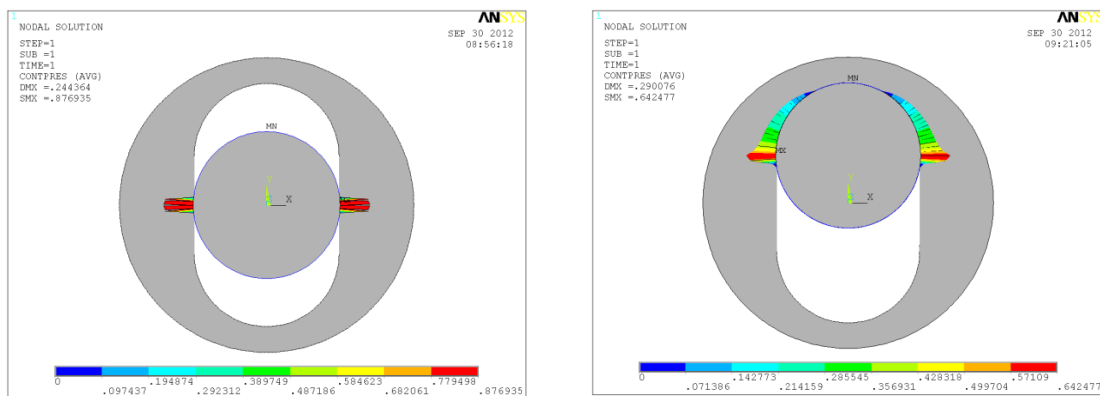


Fig. 4. Distribution of contact pressure between the rotor and stator of PCP for both their relative positions

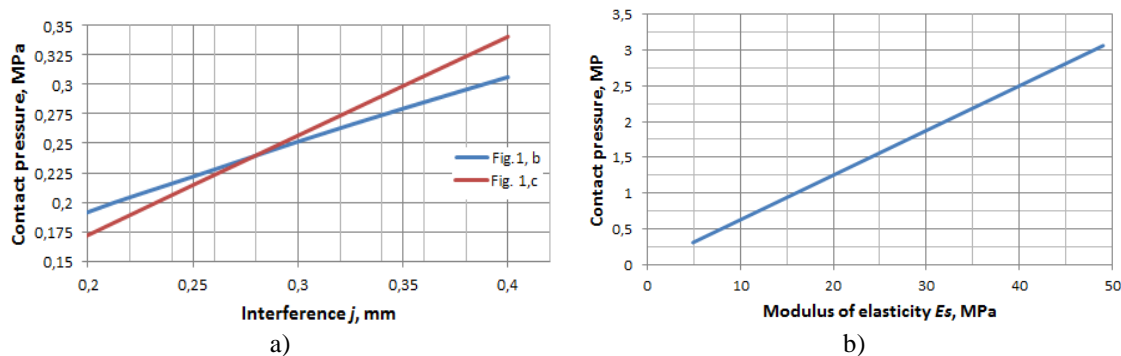


Fig. 5. a) The contact pressure vs. interference; b) The contact pressure vs. the modulus of elasticity of the stator material, E_s , for $j = 0.4$ mm interference and $\mu_s = 0.4$.

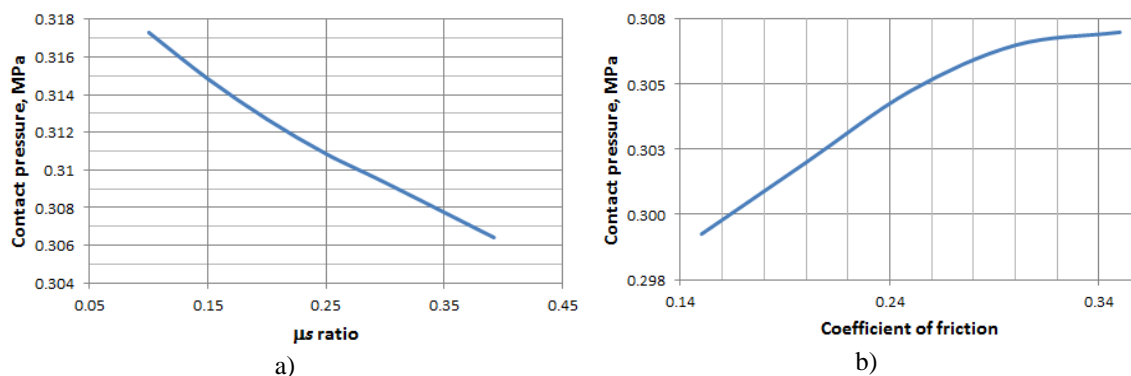


Fig. 6. a) The contact pressure vs. the Poisson coefficient value of the material of the stator in the helical pump for 0.4 mm interference and $E_s = 4.9$ MPa; b) The contact pressure vs. the value the coefficient of friction between the materials of the rotor and of the stator for 0.4 mm interference and $E_s = 4.9$ MPa of the stator material.

References

1. Selma, F., Andrade, J., Carvalho, S. – *Asymptotic approach for modelling progressive cavity pumps performance*, Asociación Argentina de Mecánica Computacional, 2010.
2. Vetter G., Wirth, W. – *Understand Progressing Cavity Pumps Characteristics and Avoid Abrasive Wear*, *Proceedings of the 12th International Pump Users Symposium*, Houston, 1995.

Analiza contactului dintre rotorul și statorul pompelor volumetrice

Rezumat

Un rol important în durata de funcționare a pompelor volumetrice, în parametrii proiectați, îl are uzura rapidă, în principal a statorului acestor echipamente. Pe lângă caracteristicile tribologice ale cuplului de materiale stator-rotor o importanță deosebită o are și presiunea de contact dintre cele două elemente în mișcare relativă. Inițial această presiune de contact este strâns legată de tipul ajustajului rotor-stator, dar ea mai depinde și de alți factori ca de exemplu: modulul de elasticitate longitudinală al materialului statorului precum și coeficientul lui Poisson al acestuia, de coeficientul de frecare etc. Din această cauză este necesar să se evalueze cu destulă precizie presiunea de contact între stator și rotor. În lucrare sunt prezentate rezultatele obținute pentru presiunea de contact, în urma unei analize numerice bazată pe FEM, în funcție de strângere și de caracteristicile fizico-mecanice ale materialului statorului pompei.